NEUTRON FIELD MEASUREMENTS AT HIGH ENERGY PROTON ACCELERATORS

T. Suzuki, M. Noguchi, Y. Oki, T. Miura, S. Miura, H. Tawara,
S. Ban, H. Hirayama, K. Kondo

National Laboratory for High Energy Physics
Oho 1-1, Tsukuba, Ibaraki, 305 Japan

L. Moritz

TRIUMF, 4004 Wesbrook Mall, Vancouver, B.C. Canada, V6T 2A3

1. INTRODUCTION

A revised law of Japanese Radiation Protection has been carried into effect on April 1st, 1989. Since, under the new law, the dose equivalent (DE) of neutron must be evaluated with double the quality factor (QF), it is necessary for the most of facilities concerned with neutron dosimetry to review the neutron DE with the new QF.

Normally, neutron personnel monitoring is carried out with many types of systems: thermo-luminescent (albedo and direct-interaction type), film, recoil or fission track, and so on. In the case of field monitoring, moderating type detectors, which consist of BF_3 proportional counter and several types of polyethylene moderator, are commonly employed. These personnel and field monitoring dosimeters are quite useful as long as the calibration is properly done for neutron field to be monitored. Hence, the information of neutron energy spectrum is essential to get the meaningful dose from these dosimeters. Also, in the scheme of the new Radiation Protection Law, a table of the fluence to DE factors for neutrons is given and, once, the energy spectrum is obtained, the DE can be calculated directly.

At high energy proton accelerators, stray neutrons are produced mostly at target stations for secondary beam lines and beam dumps. Also, small amount of stray neutrons are produced by a beam loss along the beam lines. Most of these neutrons are stopped by thick

shields and stray neutrons after penetrating through shields have widely varying energies from thermal to nearly the accelerated proton energies. Stevenson[1] has calculated proton, neutron, and charged pion spectra generated by protons of 30 GeV. From his results, the neutron energy spectrum has a peak around the energy of 100 MeV in both of the forward and lateral directions. The neutron spectrum outside shields at a high energy proton accelerator has been discussed by O'Brien.[2] His calculation shows that low energy neutron fluxes in a thick shield decrease faster than high energy neutron fluxes, and the structures of neutron energy spectrum in the high energy region have the similar shape to the spectrum of neutrons produced at the target. Thus, even outside the thick shield at a high energy proton accelerator, it is expected that a peak around 100 MeV appears in the neutron energy spectrum. This supported by the work of K.B.Shaw et al.,[3] whosummarized the neutron spectra around high energy proton accelerators.

Although it is not simple to measure the energy spectrum of stray neutrons around high energy accelerators due to the wide energy ranges, the Bonner sphere spectrometer (BSS)[4] has been successfully applied. In this work, the BSS and activation detectors were employed to obtain neutron energy spectra outside the shield of the EP2 proton beamline in the KEK counter hall. The detail of this work has been submitted to Health Physics by L.E.Moritz et al.[5] In this paper, adding four new data to their work, measurements of the spectrum and the results will be discussed.

2. EXPERIMENTAL

2-1. NEUTRON SOURCE

The extracted beam from the 12 GeV proton synchrotron is redirected into 3 beam lines, EP2-A, B and C, by a switching magnet. These beams pass through meson production targets for the secondary beam lines and are stopped at the beam dumps. Neutrons are produced mostly at the switch yard, the production targets and the beam dumps. Shields, which consist of iron, heavy concrete and ordinary

concrete, are quite thick at these locations and the energy spectrum of stray neutrons outside the shields show a typical $\sim 1/E$ dependence.

2-2. DETECTOR SYSTEM

The BSS (LUDLUM MEASUREMENTS, INC. MODEL 42-5) consisted of a 4 mm ^{6}LiI(Eu) scintillator coupled to a photomultiplier tube and of 7 polyethylene spheres of different diameters: 51mm(2"), 76mm (3"), 127mm(5"), 203mm(8"), 254mm(10"), 305mm(12"), and 457mm(18"). Also together with these spheres, the bare detector and the detector covered by Cd of 2mm thick were used.

The response functions employed in our unfolding have been calculated by Awschalon and Sanna[6] up to a neutron energy of 400 MeV. Furthermore, from 400 Mev to 10 GeV, the response functions were simply extended by a linear extrapolation.

Since all the functions at higher energy show similar response, the BSS is insensitive for neutrons of energy greater than 20 MeV. Commonly, in order to supplement the higher energy region, a carbon activation detector, which utilizes the $^{12}C(n,2n)^{11}C$ reaction with a threshold energy of approximately 20 MeV, has been applied. The cross section up to an energy of 40 MeV was taken from McLam et al.[7] Above 40 MeV, it has almost a constant value of 22 mb as shown from the work of Garber and Kinsey[8] and this number was assumed at the higher energy region. Our carbon activation detector was made of 2700g of graphite in a shape of well 150mmϕ x127mm with a hollow of 76mmϕ x76mm.

The response functions employed in our unfolding calculations and experimental set-up including the geometry of the graphite are found in a reference 5.

2-3. MEASUREMENTS

The ^{6}LiI(Eu) scintillator produces large light output through the $^{6}Li(n,\alpha)^{3}H$ reaction with Q=4.8 MeV. Although the light output showed a clear peak on a multichannel analyzer (MCA) in a neutron dominant field, for the case of mixed field, γ rays also produced

a significant light output and the subtraction of back ground (BG) from the neutron peak was necessary. Especially, this subtraction was important for the Cd cover run in a mixed field. For the most of runs with BSS spheres, the net number after the subtraction of BG and simple count rates of a single channel analyzer (SCA) were almost equal. Our activation detector system of carbon consisted of graphite, NaI counter with a size of 76mmϕ x76mm and a MCA. The amplified output of NaI was fed into a MCA and the positron annihilation gamma-ray with the energy of 0.51MeV was counted. The efficiency of the detector was calculated to be 4.8% by a Monte Carlo calculation and checked by measurements using ^{22}Na dissolved in a water mock-up of the activation detector.

Since the stray field outside shielding was not constant during the measurements, in order to normalize each BSS run, output pulses from a DE meter (Neutron Dose Rate meter, Model 2202D, manufactured by Studsvik AB Atomenergi, Sweden, and commonly called rem counter) were counted simultaneously by a scaler.

2-4. LOCATIONS

For our measurements of neutron energy spectrum, 10 typical locations were chosen and labeled as B-1 through B-10. Characteristics of the locations are summarized in Table 1. Figures from 1(a) to 1(e) show the illustrations of the locations.

3. RESULTS AND DISCUSSIONS

The multisphere data at various locations are listed in Table 2 in units of counts per second. The data of each spectrum are normalized to the average of count rates of rem counter (RC). The data of activation detector and RC are shown in units of Bq/atom and μSv/h, respectively.

Figure 2 illustrates the normalized multisphere data listed in Table 1. Since the location of B-6 was located in the counting house area, the radiation level must be controlled quite low. In the figure, it has been shown that counting rates of B-6 in small

spheres and bare detector are larger than other spectra and, hence, the neutron spectrum at this location is soft as expected. On the other hand, the B-4 spectrum has lower counting rates in small spheres and is thought to be harder than other spectrum. The reason of the hardness is that the measuring points B-4 is located down stream of KO production target and KO beam dump, where high energy neutrons are produced towards the location.

3.1 NEUTRON SPECTRUM UNFOLDING

Using the data listed in Table 2, neutron spectra were unfolded with the iterative non linear unfolding code LOUHI78.[9] Normally, a 1/E shape is a good approximation for an energy spectrum outside shields and the shape is assumed as a trial solution.

Three neutron spectra at B-1, B-2 and B-6 are shown in Fig. 3. The location B-2 was near the proton beam switch yard and a high radiation level was observed. A spectrum at B-6 shows a typical 1/E shape and the radiation level of neutron and γ ray was lower than 1 μSv/h. All spectra except B-6 show two peaks at neutron energies around 1 and 100 MeV. These peaks are well illustrated in Fig. 4, which is expressed in lethargy. A peak around 1 MeV is due to evaporation process and, as discussed by O'Brien et al.,[2] another peak around 100 Mev is considered to be due to the penetration of high energy neutrons.

Table 3 shows comparison between measurements and the unfolding results in units of μSv/h. Results of unfolding calculations are shown together with fitting errors for three cases; unfolding with full data set, without 18" data, and without ^{11}C data. Since Moritz et al.[5] showed that an analytic formula of Thomas (TH65)[10] and a table given in ICRP-51[11] gave typical results, using the energy spectrum at each location, a DE was estimated with these two factors. Comparing fitting errors of LOUHI code, errors of calculation with the full data set are bigger than other two cases. Especially, without ^{11}C data, the errors become small. For the most of cases, including 25% of ^{11}C data, the minimum of the fitting error is obtained. At this minimum, the DE is almost 30% less than the calculation with the full data set.

At a high energy accelerator facility, three major particles, protons, neutrons and pions, contribute to the production of ^{11}C from ^{12}C. From the calculation of Stevenson[1], few charged particles can penetrate through thick shields in the lateral direction but, in the forward direction, it is plausible that some fraction of charged particles penetrate through shields as discusse by Moritz et al.[5] However, even in the case of the B-4 spectrum of the forward direction, the fitting error gets minimum with 25% of ^{11}C data and the ^{11}C dependence of the error is similar to other spectrum in the lateral direction. Hence the results of calculation with full data set are used for a DE comparison between the measurements and the unfolding results.

When a BSS is applied to measure a neutron spectrum, a sphere of 18" is often not employed. From Table 3, the DE without 18" data is bigger than the DE with full data set by 50 to 100%. Without information of a 18" sphere, the activation data seems to be emphasized and the high energy component in the spectrum increases. As seen from the characteristics of response functions of each ball,[6] the response of 18" sphere is sensitive for neutron energy above 1 MeV and the data has a function of reducing the component higher than 20 MeV.

Moritz et al.[5] also discussed that normalized unfolding spectra obtained from data of Table 2 agreed well with a result of analytic calculation by O'Brien et al.[2]

3.2 DOSE EQUIVALENT COMPARISON

Readings of a RC is reliable for neutron below $\sim$10 MeV and a graphite activation detector has a response to neutron above 20 MeV. Thus, for the purpose of field monitoring, it is considered that, at a high energy accelerator, the sum of RC and activation detector gives the radiation level. Considering that a RC has a response even for neutron above 20 MeV, the sum seems to give larger radiation level than the level expected from the field, which is better from the point of view of radiation control.

From Table 3, it is clear that most of the sum is always larger than unfolding results calculated with ICRP dose equivalent

conversion factor. However, the results from the TH65 formula, most of which are twice as many as those from the ICRP table, almost equal to the sum. Thus, a DE is severely affected by the conversion factors and it is important to have the reliable conversion factor for the meaningful occupational monitoring.

4. CONCLUSION

Since stray neutrons outside shields at a high energy proton accelerator have energies from thermal to the accelerated proton energy, it is not simple to measure the energy spectrum. In this report and a work 5 by Moritz et al.[5], a multisphere technique with carbon activation has been discussed to obtain the spectrum. The results agree well with the calculation of O'Brien et al. and a DE deduced from the spectrum is also comparable with our regular field monitoring using a DE rem counter. In our measurements, as expected from the work of Stevenson[1] and O'Brien et al.,[2] higher energy neutrons than 20 MeV, which have the peak around 100 MeV, have been observed and contributes 50% to the DE. As a result, it seems reasonable that, in our regular field monitoring with a rem counter, readings of the counter are doubled to evaluate the radiation level in μSv/h.

REFERENCES

(1)G. R. Stevenson, Health Physics 47(1984) pp837-847
The estimation of dose equivalent from the activation of plastic scintillators

(2)K. O'Brien and J. E. McLaughlin, Nuc. Ins. Methods 60(1968) pp129-140
The propagation of the neutron component of the nucleonic cascade at energies less than 500MeV: Theory and solution to the accelerator transverse shielding problem

(3)K. B. Shaw, G. R. Stevenson and R. H. Thomas, Health Physics 17(1969) pp459-469
Evaluation of dose equivalent from neutron energy spectra

(4)R. L. Bramblett, R. I. Ewing and T. W. Bonner, Nuc. Ins. Methods 60(1968) pp1-12
A new type of neutron spectrometer
(5)L. E. Moritz, T. Suzuki, M. noguti, Y. Oki, T. Miura, S. Miura, H. Tawara, S. Ban H. Hirayama and K. Kondo.
Submitted to Health Physics, KEK Preprint 88-95
Characteristics of the neutron field in the KEK counter hall
(6)M. Awschalom and R. S. Sanna, Radiation Protection Dosimetry 10(1985) pp 89-101
Applications of Bonner sphere detectors in neutron field dosimetry
(7)V. McLam, C. L. Dunford, and P. F. Rose, Neutron Cross Sections 2(1988)p35
(8)D. I. Garber and Kinsey, Neutron Cross Sections, 3rd ed. vol 2(1976)
(9)J. T. Routti and J. V. Sandverg, TKK-F-A358(1978)
Unfolding techniques for activation detector analysis
J. T. Routti and J. V. Sandverg, TKK-F-A359(1978)
General purpose unfolding program LOUHI78 with linear and nonlinear regularization
(10)R. H. Thomas, The radiation fields observed around high energy accelerators, Proc. of XI International Congress of Radiology, Rome, Italy:1965
(11)International Commission on Radiation Protection, Data for use in protection against external radiation,
Annals of the ICRP, ICRP 17, No. 2/3:1987

TABLE 1

Characteristics of locations for measurments
(These locations are shown in Fig. 1(a) through Fig. 1(e))

Location	Characteristics of location
B-1	Near the switchyard of proton beam and about 4m away from shields
B-2	Near the switchyard of proton beam and beside shields
B-3	Beside shields along the EP2-C beam line and near production target
B-4	Down stream of KO production target and KO beam dump
B-5	Small gap between shields along the EP2-B beam line
B-6	Working area for experiment
B-7	Down stream of $\pi \cdot \mu$ beam line
B-8	Top of shields and down stream of the switchyard of proton beam
B-9	Top of shields and just above the switchyard of proton beam
B-10	Beside shields along the EP2-A beam line and near the switchyard

TABLE 2

Results of the multisphere and carbon activation measurements.
The multisphere measurments are in units of counts per second.

	Location/Spectrum									
Detector	B-1	B-2	B-3	B-4	B-5	B-6	B-7	B-8	B-9	B-10
Cd	0.19	0.92	0.08	0.20	0.39	0.03	0.01	0.10	0.08	0.26
Bare	0.70	3.84	0.23	0.35	2.55	0.05	0.07	0.75	0.57	1.65
2"	1.44	7.96	0.55	1.52	4.04	0.09	0.14	1.20	0.92	3.02
3"	2.54	12.1	0.84	2.95	5.68	0.14	0.22	1.55	1.36	4.68
5"	3.87	15.0	0.98	4.51	7.32	0.18	0.28	1.89	1.80	5.94
8"	3.17	12.4	0.87	4.32	5.96	0.12	0.21	1.36	1.57	3.95
10"	2.21	9.63	0.70	3.45	4.57	0.08	0.13	1.08	1.23	2.59
12"	1.63	7.10	0.43	2.78	3.36	0.05	0.11	1.82	0.96	1.91
18"	0.86	3.56	0.23	1.80	1.37	0.02	0.05	0.55	0.58	1.25
^{11}C*	450.	2460.	70.	1400.	730.	----	30.	270.	200.	340.
Rem Counter**	20.	80.	5.8	43.	34.	0.6	1.2	10.	13.	44.

* in units of Bq/atom x 10^{-27} at saturation

** in units of μSv/h

TABLE 3

Dose equivalent comparison between measurements and unfolding results with LOUHI code. The fluence to dose equivalent conversion is made with the analytic formula (TH65) of Thomas and a table given in ICRP-51 (ICRP-slab). A flux to dose equivalent rate conversion factor for the $^{12}C(n,2n)C^{11}$ is 1 $cm^{-2}s^{-1}$ equal to 0.1 $mrem \cdot h^{-1}$(28fSvm^2).

Dose Equivalent Rate in units of μSv/h

Spectrum		B-1	B-2	B-3	B-4	B-5	B-6	B-7	B-8	B-9	B-10
Rem Counter		20.	80.	5.8	43.	34.	0.6	1.2	10.	13.	44.
^{11}C ( )20MeV)		21.	110.	3.	64.	33.	----	1.5	13.	9.	16
Rem + ^{11}C		42.	190.	8.8	107.	67.	0.6	2.7	23.	22.	60.
UNFOLDING	with full data										
	ICRP-slab	27.	110.	6.6	48.	52.	---	1.6	13.	16.	36.
	TH65	46.	190.	11.	87.	90.	---	2.8	21.	28.	66.
	Fit. Error(%)	12.	12.	9.5	11.	8.7	---	11.	5.6	8.6	10.
	without ^{11}C data										
	ICRP-slab	18.	71.	4.7	30.	36.	0.6	1.1	10.	10.	25.
	TH65	24.	93.	6.2	41.	49.	0.7	1.5	14.	14.	36.
	Fit. Error(%)	7.0	3.2	6.3	4.9	4.8	12.	4.0	5.0	4.1	6.4
	without 18" data										
	ICRP-slab	33.	150.	7.0	28.	58.	0.6	2.2	13.	18.	42.
	TH65	61.	300.	12.	36.	103.	0.7	4.3	22.	33.	84.
	Fit. Error(%)	10.	9.0	8.0	14.	7.4	13.	8.3	5.6	6.9	9.6

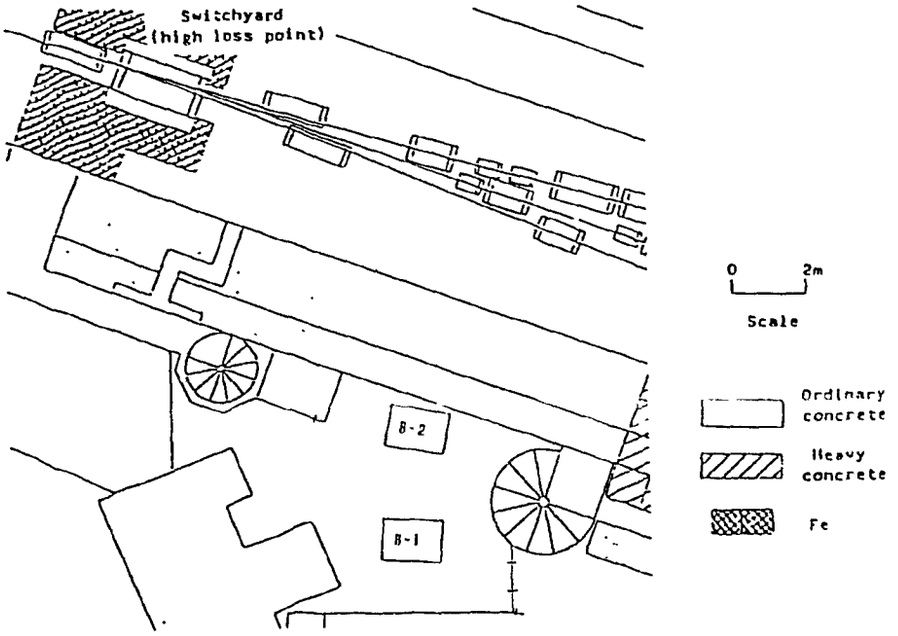

Fig. 1(a) Mesurement's locations. B-1 and B-2

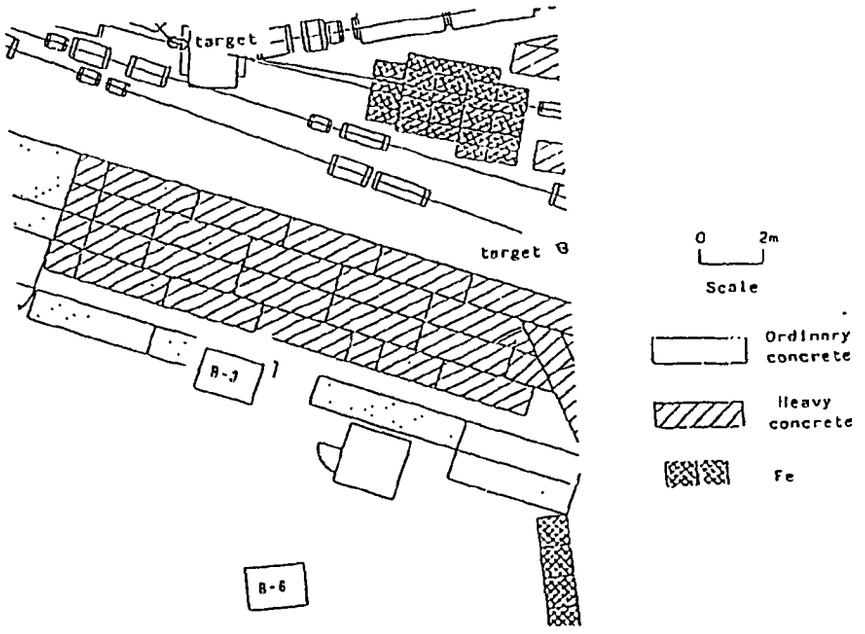

Fig. 1(b) Mesurement's locations. B-3 and B-6

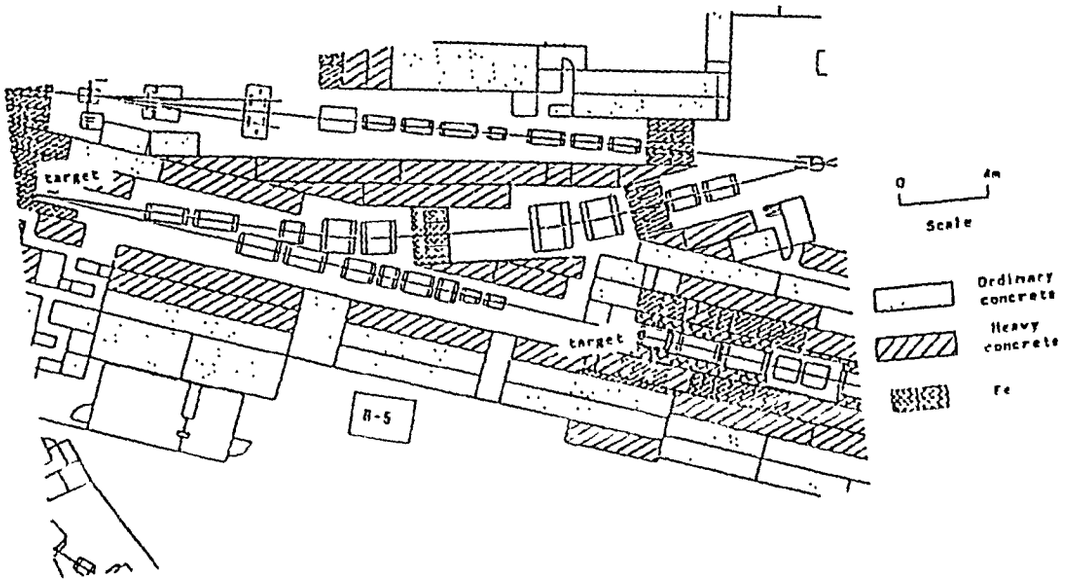

Fig. 1(c) Mesurement's location , B-5

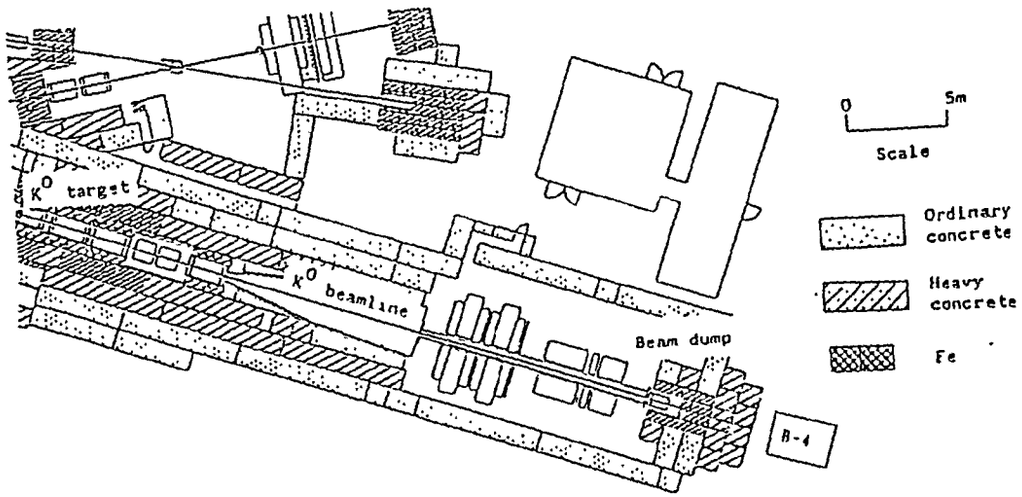

Fig. 1(d) Mesurement's location , B-4

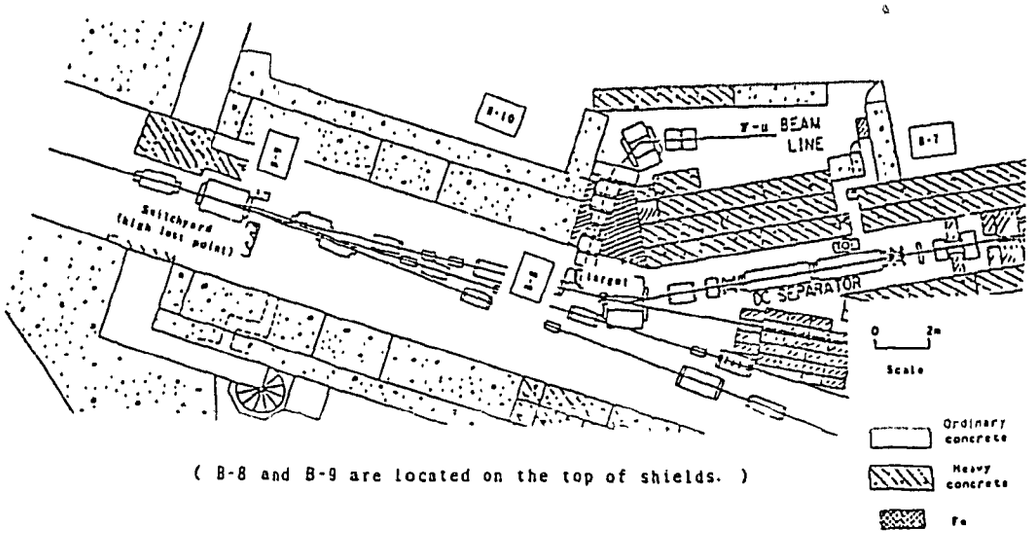

Fig. 1(e) Mesurements' locations, B-7, B-8, B-9, and B-10

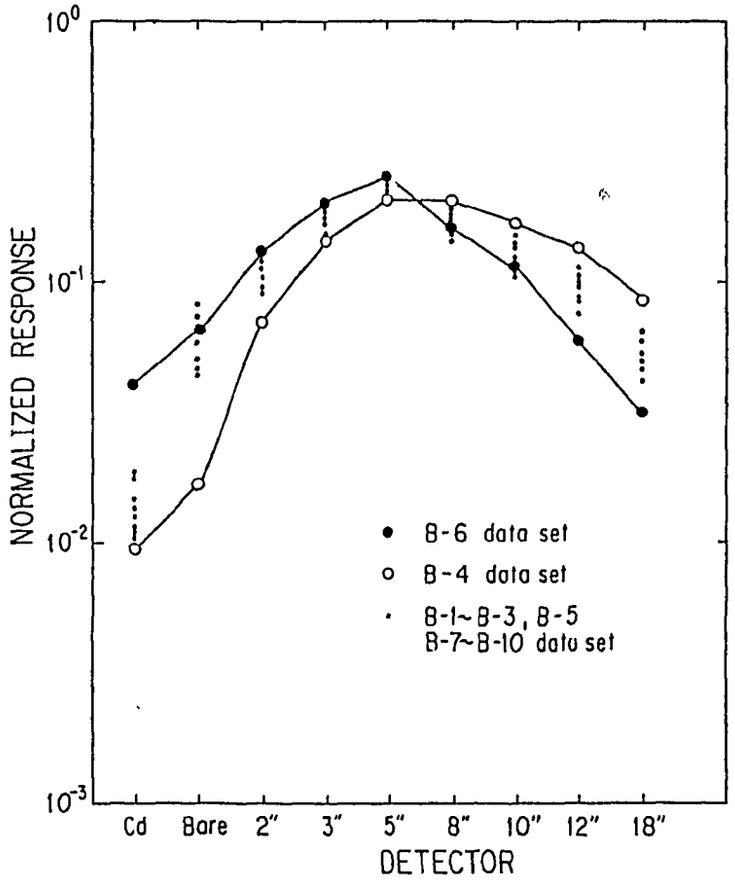

Fig. 2 Normalized multisphere data

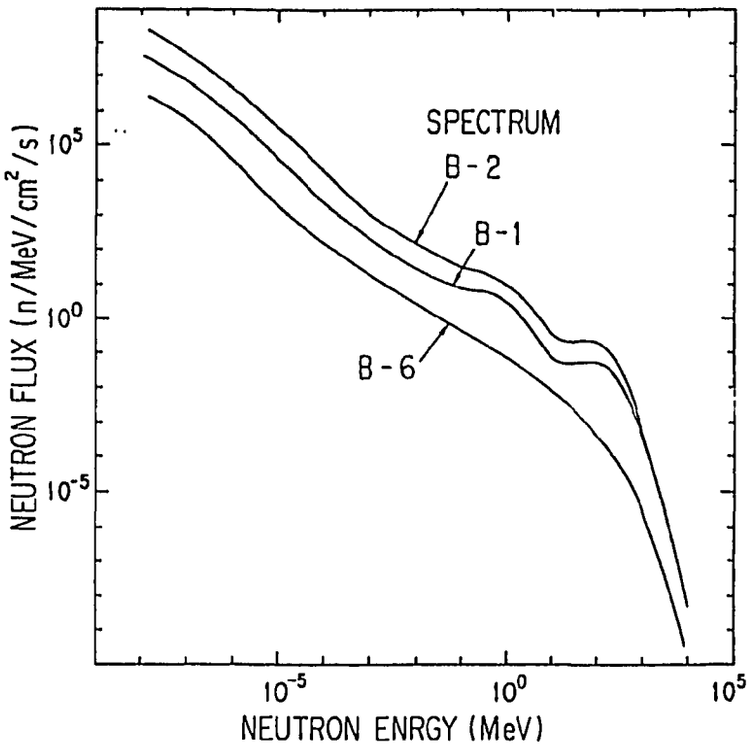

Fig. 3 Neutron energy spectrum at B-1, B-2 and B-6

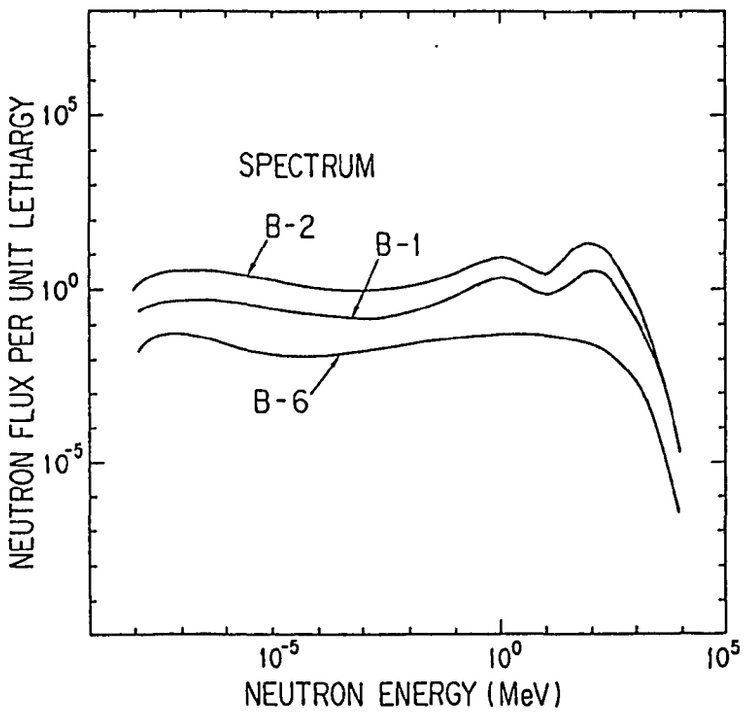

Fig. 4 Lethargy plot of same spectra as in Fig. 3